Journal of Medicinal Chemistry

Article

pubs.acs.org/jmc

Pyridyl Benzamides as a Novel Class of Potent Inhibitors for the Kinetoplastid *Trypanosoma brucei*

Lori Ferrins,[†,□] Michelle Gazdik,[∥,⊥,□] Raphaël Rahmani,[†] Swapna Varghese,[∥] Melissa L. Sykes,[#] Amy J. Jones,[#] Vicky M. Avery,[#] Karen L. White,[‡] Eileen Ryan,[‡] Susan A. Charman,[†,‡] Marcel Kaiser,[▽,○] Christel A. S. Bergström,[§,◆] and Jonathan B. Baell*[,†,⊥,¶]

[†]Medicinal Chemistry, [‡]Centre for Drug Candidate Optimisation, and [§]Drug Delivery, Disposition and Dynamics, Monash Institute of Pharmaceutical Sciences, Monash University, Parkville, Victoria 3052, Australia

[∥]Department of Chemistry, La Trobe Institute for Molecular Science, La Trobe University, Melbourne, Victoria 3086, Australia

[⊥]The Walter and Eliza Hall Institute, 1G Royal Parade, Parkville, Victoria 3052, Australia

[#]Eskitis Institute for Drug Discovery, Griffith University, Brisbane Innovation Park, Don Young Road, Nathan, Queensland 4111, Australia

[▽]Swiss Tropical and Public Health Institute, Socinstrasse 57, Basel, 4051, Switzerland

[○]University of Basel, Petersplatz 1, Basel, 4003, Switzerland

[◆]Department of Pharmacy, Uppsala University, Biomedical Center P.O. Box 580, SE-751 23 Uppsala, Sweden

[¶]Department of Medical Biology, University of Melbourne, Parkville, Victoria 3010, Australia

Supporting Information

ABSTRACT: A whole-organism screen of approximately 87000 compounds against *Trypanosoma brucei brucei* identified a number of promising compounds for medicinal chemistry optimization. One of these classes of compounds we termed the pyridyl benzamides. While the initial hit had an IC_{50} of 12 μM, it was small enough to be attractive for further optimization, and we utilized three parallel approaches to develop the structure−activity relationships. We determined that the physicochemical properties for this class are generally favorable with particular positions identified that appear to block metabolism when substituted and others that modulate solubility. Our most active compound is **79**, which has an IC_{50} of 0.045 μM against the human pathogenic strain *Trypanosoma brucei rhodesiense* and is more than 4000 times less active against the mammalian L6 cell line.

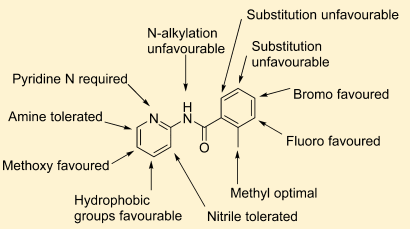

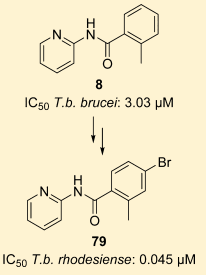

INTRODUCTION

Human African trypanosomiasis (HAT) currently affects more than 20000 people according to the latest report published by the World Health Organization.[1] HAT is caused by the transmission of *Trypanosoma brucei* spp. by the tsetse fly to humans, and, as a result, this disease is largely restricted to Africa where the vector, parasite, and animal reservoirs coexist.[2] Infection is with either *Trypanosoma brucei gambiense* or *Trypanosoma brucei rhodesiense*, and the rate of progression of the disease is subspecies-dependent, with *T.b. gambiense* being accountable for 95% of cases and causing a chronic infection, while *T.b. rhodesiense* presents as an acute infection.[2] The disease has two stages: the first stage is the hemolymphatic phase where trypanosomes multiply in subcutaneous tissue, blood, and the lymphatic system, and is accompanied by fever, headaches, joint pain, and itching.[2] Stage two is the neurological phase and occurs when the parasites cross the blood brain barrier (BBB) and infect the central nervous system (CNS). This typically results in behavioral change, confusion, poor coordination, and sleep disturbances.[2] Without treatment HAT is eventually fatal. There are currently few treatment options, making this disease a key target for drug discovery.

For treatment of the first stage of HAT, there are currently two drugs registered for use, as shown in Figure 1: pentamidine (**1**) and suramin (**2**). Pentamidine is used to treat infection with *T.b. gambiense*,[3] while suramin is prescribed to patients infected with *T.b. rhodesiense*.[4,5] Neither of these drugs can cross the BBB, and they both have significant side effects. Pentamidine has been associated with nephrotoxicity and diabetes mellitus,[6] while suramin can lead to renal failure and exfoliative dermatitis.[4] Melarsoprol (**3**) was the first drug used to treat stage two HAT.[6,7] It is effective against both pathogenic subspecies, although recently resistance to the drug has been observed.[7] There are also significant side effects associated with its use including reactive encephalopathy, which can be fatal in

Received: February 4, 2014

   dx.doi.org/10.1021/jm500191u | *J. Med. Chem.* XXXX, XXX, XXX−XXX

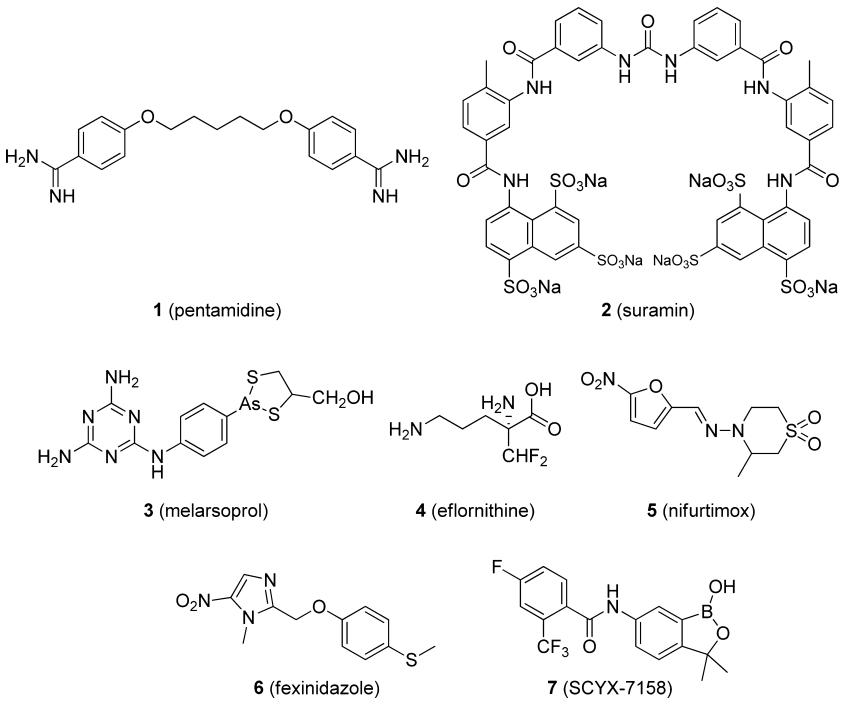

Figure 1. Drugs used for the treatment of human African trypanosomiasis (**1**–**5**), fexinidazole (**6**), now in phase II/III clinical trials, and SCYX-7158 (**7**) currently in phase I clinical trials.

3–10% of patients.[7] Eflornithine (**4**), effective against *T.b. gambiense*,[7] was registered in 1990 and is less toxic than its predecessor. More recently, a combination therapy of nifurtimox (**5**) and eflornithine (**4**) (NECT) was introduced, but it is ineffective against *T.b. rhodesiense* and the need for parenteral administration is a drawback.[8] A number of compounds have recently entered clinical development for HAT. Pafuramidine, a constrained analogue of pentamidine, entered clinical development in 2005 but was abandoned when liver toxicity and delayed renal insufficiency were identified in an extended phase 1 trial.[9] Drugs currently in clinical trials are fexinidazole (**6**), a nitroheterocycle that is in phase II/III clinical trials,[10] and the oxaborole, SCYX-7158 (**7**), which entered phase I trials in March 2012. The outcome of these trials is pending.[11]

Fortunately, with the advent of recent public–private partnerships and related initiatives,[1] it is anticipated that improved treatments will emerge for many of the so-called "neglected" diseases. There are a number of drug discovery avenues currently being utilized in the search for new antitrypanosomal drugs, which we have recently reviewed.[12] We recently conducted high-throughput screening (HTS) against *T. brucei* using a library of 87296 compounds, and discovered several classes with promising activity.[13] One of these has been progressed to a hit-to-lead medicinal chemistry optimization program.[14] Some inhibitor series were not discussed in the initial HTS publication because they did not meet predefined selection criteria. One of these was a simple pyridyl benzamide (**8**), which was slightly less active than the other classes with an IC_{50} value of 12 μM, close to the predefined activity cutoff value of <10 μM, and a selectivity index (SI) of 28 relative to HEK 293 cells. However, this compound was attractive to the medicinal chemists as an optimization candidate as its physicochemical properties were deemed to be favorable for development (Figure 2).

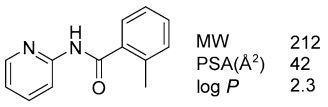

Figure 2. Structure and physicochemical parameters of screening hit **8**.

Compound **8** possesses a very low molecular weight of 212 g mol^{-1}, a low polar surface area of 42 $Å^2$ suitable for potential CNS penetration to treat stage two HAT, an attractively low lipophilicity (log *P* of 2.3), and would be neutral at physiological pH, aiding BBB penetration. The low molecular weight results in a high ligand efficiency and much scope to optimize; as such, this compound was selected for development of structure–activity relationships (SAR). Herein, we report the results of this investigation.

RESULTS AND DISCUSSION

Mining the HTS database returned 15 compounds, which were broadly related to **8**. However, these compounds were not sufficiently similar to develop meaningful SAR. Three parallel approaches were then employed to establish a focused SAR investigation. The first of these involved identification of close analogues in the literature that were associated with previously reported biological activity. Of particular interest were those compounds with demonstrated activity against trypanosomes, or whereby *T. brucei* possesses a target that the compound had reported activity against in other organisms. From this search, it was determined that relatively little was known about the biological activity of **8**, although a low level of antifungal activity against a strain of corn-smut has been reported (*Ustilago maydis*).[15] The closely related 2-methylbenzanilide system was reported to have more effective and wide ranging antifungal activity and demonstrated activity against succinate dehydrogenase (Complex II in mitrochondria) in corn smut.[15] This

dx.doi.org/10.1021/jm500191u | J. Med. Chem. XXXX, XXX, XXX–XXX

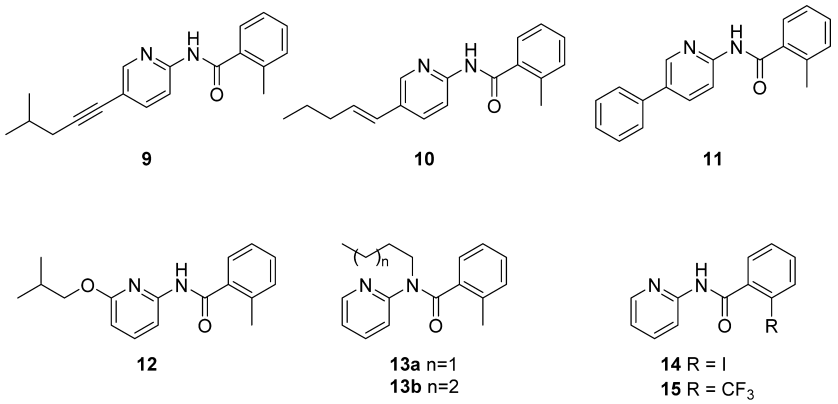

Figure 3. Potential synthetic targets identified in the literature, where pyridyl benzamides **9**–**15** are counterparts to corresponding benzanilides with associated antifungal activity.

enzyme has been previously identified in *T. brucei* procyclic trypomastigotes.[16] There is some precedence for cross-species activity of compounds toward fungi and trypanosomes.[17,18] We therefore targeted pyridyl benzamides containing groups known to impart great potency to fungal succinate dehydrogenase, in case they did so for *T. brucei* as well.[15] These compounds (**9**–**15** in Figure 3) have lipophilic groups in the 5-position (**9**–**11**) or 6-position (**12**) of the pyridine ring, or on the amide nitrogen atom (**13**), while **14** and **15** contain a 2-iodo and 2-trifluoromethyl, respectively, on the benzamide ring instead of a methyl group.

The second approach that we adopted comprised searching databases of compound biological activities such as the TCAMS set[19] and PubChem. A number of analogues were identified with a variety of biological activities. Those of particular interest were **16**–**18** (Figure 4), which were identified as active against

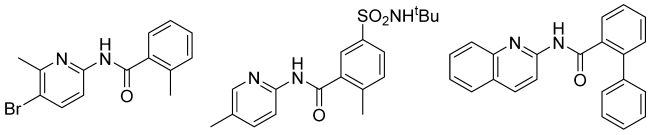

Figure 4. Compounds **16**–**18** were identified through searching PUBCHEM or the TCAMS set.

Plasmodium falciparum. These compounds therefore became synthetic targets, where any observed activity against *T. brucei* could provide information regarding a possible mode of action for these compounds.

The third approach comprised directed synthesis to develop the SAR through probing different regions of the molecule with varying substituents.

As shown in Scheme 1, the synthetic versatility of this scaffold allowed ready access to all target molecules. Core assembly was readily constructed via coupling of an appropriately substituted 2-aminopyridine with an appropriately substituted benzoic acid or benzoyl chloride. In the case of **12**, the alkoxy group was introduced prior to an amide formation in a reaction involving displacement of a labile aryl halogen with NaH-generated alkoxide in DME. Lipophilic hydrocarbon substituents in the pyridine ring such as those in **9**–**11** were introduced with Sonogashira (**9**) or Suzuki (**10**, **11**) reactions after coupling, whereas alkylation of the amide nitrogen atom readily gave **13**. In the case of **17**,

Scheme 1[a]

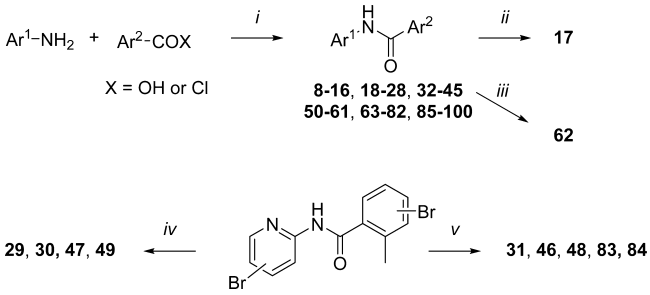

[a](i) X = OH, DIPEA, HBTU, DMF, 60 °C, or EDCI, DMAP, DMF, 25°C; X = Cl, pyridine, 16 h, 25°C; (ii) $ClSO_3H$, then $^tBuNH_2$; (iii) MeI, K_2CO_3, TBAB, acetone, 16 h, 25 °C; (iv) alkyne, CuI, PPh_3, $Pd(PPh_3)_2Cl_2/Pd(PPh_3)_4$, DMF, Et_3N, microwave 120 °C, 10–40 min; (v) boronic acid, K_2CO_3, TBAB, $Pd(PPh_3)_2Cl_2$, 1,4-dioxane, H_2O, microwave 130 °C, 15 min.

chlorosulfonylation after coupling followed by reaction with *tert*-butylamine was successful.

The biological data for **8**–**18** are shown in Table 1. Retesting of a fresh sample of **8** synthesized in-house returned a slightly

Table 1. *T.b. brucei* Inhibitory Activity of 8–18

ID	IC_{50} (μM) ± SEM	percentage inhibition at 10 μM
8[a]	3.03 ± 0.7	80%
9		12%
10		19%
11		11%
12		<10%
13a		11%
13b		17%
14		38%
15		<10%
16		<10%
17		12%
18		53%

[a]Selectivity index relative to HEK293 cells is 27.5.

improved IC_{50} (3.03 μM) than originally obtained (12 μM). It can be seen quite clearly that the structural changes in general were detrimental to activity. Our interpretation of these results is that *T. brucei* SAR for this class of compound is divergent from SAR for any other known biological activities.

dx.doi.org/10.1021/jm500191u | J. Med. Chem. XXXX, XXX, XXX–XXX

Table 2. *T.b. brucei* Inhibitory Activity of SAR Probes of 8 Focusing on the Pyridine and Amide Moieties

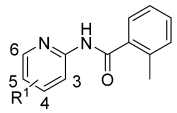
19-51

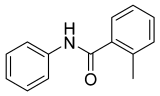
52

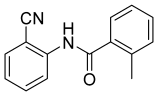
53

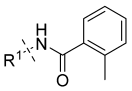
54-61

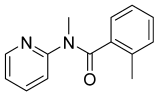
62

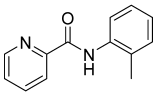
63

ID	R^1	IC_{50} (μM) ± SEM	percentage inhibition at 10 μM	SI[a]
19	3-OCH_3		<10%	
20	3-CH_3		34%	
21	3-F		<10%	
22	3-[N][b]		<10%	
23	4-CN	2.3 ± 0.04		
24	4-[N][b]		35%	
25	4-CH_3	2.1 ± 0.1		>37
26	4-Cl	2.1 ± 0.1		>38
27	4-Br	1.8 ± 0.01		>41
28	4-F	0.51 ± 0.13		168
29	4-C≡CPh	1.7 ± 0.4		>51
30	4-C≡CCH_2iPr	1.1 ± 0.08		>53
31	4-Ph	2.0 ± 0.002		31
32	5-OCH_3	3.8 ± 0.4		>22
33	5-CH_3		<10%	
34	5-F		33%	
35	5-[N][b]		<10%	
36	5-CN		<10%	
37	5-Cl		<10%	
38	5-Br		<10%	
39	6-OCH_3		<10%	
40	6-CH_3		<10%	
41	6-F		<10%	
42	6-CN		11%	
43	6-[N][b]		<10%	
44	6-Cl		<10%	
45	6-Br		<10%	
46	6-Ph		33%	
47	6-C≡CCH_2iPr		<10%	
48	6-CH=$CH(CH_2)_2CH_3$	6.0 ± 0.07		>3
49	6-C≡CPh		<10%	
50	6-OH		<10%	
51	6-NH_2	4.6 ± 0.8		>19
52			<10%	
53			<10%	
54			<10%	
55			<10%	
56			<10%	
57			<10%	
58			<10%	
59			<10%	
60			<10%	
61			<10%	
62			18%	
63			<10%	

[a]Selectivity relative to HEK293 cells. [b][N] = endocyclic nitrogen.

Much more promising were the results from exploring **8** using conventional SAR elaboration. Shown in Table 2 are the data for compounds with a focus on varying substituents around the pyridine ring.

Here it can be seen that at the 3-position, methoxy (**19**), methyl (**20**), or fluoro (**21**) were not well tolerated and neither was an endocyclic nitrogen (**22**). In the 4-position, a cyano (**23**) was tolerated, an endocyclic nitrogen (**24**) less so, but in contrast, good activity accompanied substitution with a range of hydrophobic groups (**25**−**31**), particularly with the 4-fluoro (**28**). The similar activities for the 4-chloro (**26**) and very bulky phenylacetylene (**29**) or phenyl (**31**) imply this could largely be a favorable transport effect rather than a specific interaction with a hydrophobic pocket in an intracellular target site. In the 5-position, methoxy was favorable for activity (**32**), but methyl (**33**), fluoro (**34**), chloro (**37**), bromo (**38**), nitrile (**36**), or an endocyclic nitrogen (**35**) were not. As it is hard to envisage that a methoxy would aid transport, this SAR is consistent with the methoxy interacting favorably with its target, whether it be intra- or extracellular. In contrast to substitution at the other

dx.doi.org/10.1021/jm500191u | J. Med. Chem. XXXX, XXX, XXX−XXX

Table 3. *T.b. brucei* Inhibitory Activity of a Number of Analogues of the Tolyl Ring

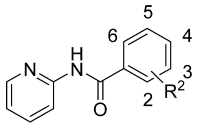

64-91

ID	R^2	IC_{50} (μM) ± SEM	percentage inhibition at 10 μM	SI[a]
64	H	9.07 ± 2.2		9.2
65	2-Et	2.74 ± 1.0		30
66	2-F		35%	
67	2-Cl		44%	
68	2-OCF_3		13%	
79	2-Ph		<10%	
70	2-CH_3, 3-F	0.89 ± 0.04		94
71	3-F	7.33 ± 2.1		11
72	2-CH_3, 3-Cl	0.63 ± 0.09		132
73	2-CH_3, 3-Br	5.7 ± 0.2		15
74	2-CH_3, 3-CH_3	3.5 ± 0.2		24
75	2-CH_3, 3-OCH_3		10%	
76	2-CH_3, 3-[N][b]		21%	
77	2-CH_3, 4-F	1.9 ± 0.3		44
78	2-CH_3, 4-Cl	1.1 ± 0.09		76
79	2-CH_3, 4-Br	1.1 ± 0.06		60
80	2-CH_3, 4-OCH_3		<10%	
81	2-CH_3, 4-CH_3	0.98 ± 0.07		85
82	2-CH_3, 4-CH=CH$(CH)_2CH_3$		24%	
83	2-CH_3, 4-Ph		<10%	
84	2-CH_3, 5-F		<10%	
85	2-CH_3, 5-Br		<10%	
86	2-CH_3, 5-CH_3		22%	
87	2-CH_3, 5-OCH_3		<10%	
88	2-CH_3, 5-[N][b]		<10%	
89	2-CH_3, 6-CH_3		<10%	
90	2-CH_3, 6-F		45%	
91	2-CH_3, 6-[N][b]		12%	

[a]Selectivity relative to HEK293 cells. [b][N] = endocyclic nitrogen.

positions, no favorable substitution could be found for the 6-position, even after extensive probing with a variety of diverse groups (**39**–**51**). Perhaps the only exception was **51**, where an amino group appeared to be tolerated with an IC_{50} of 4.6 μM. Removal of the pyridyl nitrogen as with the benzanilide (**52**), and the substitution of the pyridine ring with a range of five-membered heterocycles (**54**–**61**), resulted in the complete loss of activity and demonstrated that the pyridine ring was essential for activity. It was thought that replacement of the pyridinyl nitrogen with a nitrile (**53**) could overcome the observed loss of activity as nitriles are known to replace water-mediated hydrogen-bond bridges involving heterocyclic nitrogens,[20] although here such a change resulted in loss of activity. Finally, it was determined through inactivity of the *N*-methyl (**62**) and reverse amide (**63**) analogues that the secondary amide was essential for activity.

The SAR for the tolyl ring was probed next, and the results are shown in Table 3.

Here, it is observed that the methyl group is important, and its loss (**64**) led to a 3-fold decrease in activity as compared to **8**. Interestingly, extension of the 2-methyl to a 2-ethyl was well tolerated, with **65** having an IC_{50} of 2.74 μM, although fluoro (**66**), chloro (**67**), trifluoromethoxy (**68**), and phenyl (**69**) were not tolerated, complementing the results for **14** and **15** in Table 1. Maintaining the 2-methyl group, other positions were probed, and it can be seen that while a 3-methoxy (**75**) or endocyclic nitrogen (**76**) were not tolerated, a 3-fluoro (**70**) was highly favorable for activity with an IC_{50} of 0.89 μM. The methyl group was confirmed to be important as its loss from **70** to give des-methyl analogue **71** led to a near 10-fold loss of activity. Substitution with 3-chloro (**72**) was favorable with an IC_{50} of 0.63 μM, while the 3-methyl (**74**) and 3-bromo (**73**) were significantly less active with respective IC_{50} values of 3.5 and 5.7 μM. This suggests that a small, electron-withdrawing and hydrophobic group is favorable for activity at the 3-position. In the 4-position, a methoxy (**80**) was not tolerated; fluorine (**77**), chlorine (**78**), bromine (**79**), and methyl (**81**) substitution all gave favorable results, with IC_{50} values of 1.9, 1.1, 1.1, and 0.98 μM, respectively. In the 5-position, substitution of an endocyclic nitrogen (**88**) led to a loss of activity, and similarly fluorine (**84**), bromine (**85**), methyl (**86**), and methoxy (**87**) in this position rendered the compounds inactive. It appears as though this position nestles tightly within the target's active site and no manipulation is possible. Likewise, substitution at the 6-position was unfavorable for activity with methyl (**89**), fluorine (**90**), and an endocyclic nitrogen (**91**) leading to a complete loss of activity.

dx.doi.org/10.1021/jm500191u | J. Med. Chem. XXXX, XXX, XXX–XXX

Finally, we looked for evidence of additive SAR to see if further increases in potency could be engineered in a rational way. We saw previously (Table 3) that when R^2 was 2-methyl, 3-fluoro (**70**) or 2-methyl, 4-fluoro (**77**), respective IC_{50} values of 0.89 and 1.9 μM were obtained, which were better than that for **8** (3.03 μM). Combining the 2-methyl, 3-fluoro, and 4-fluoro in the one molecule gave a further improvement in activity, and **92** (Table 4) returned an IC_{50} of 0.41 μM. We also

Table 4. *T.b. brucei* Inhibitory Activity of Compounds with a Combination of Favorable Substitution Patterns around the Pyridyl and Phenyl Rings in Search of Additive SAR

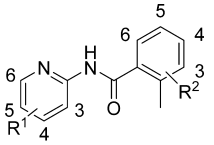

92-100

ID	R^1	R^2	IC_{50} (μM) ± SEM	SI[a]
92	H	3-F, 4-F	0.41 ± 0.07	205
93	4-CH_3	3-F	0.83 ± 0.01	100
94	4-CH_3	3-F, 4-F	0.90 ± 0.44	93
95	4-Cl	3-F	0.47 ± 0.05	177
96	4-Cl	3-F, 4-F	0.53 ± 0.26	160
97	4-F	3-F	0.10 ± 0.04	851
98	4-F	3-F, 4-F	0.19 ± 0.24	450
99	5-OCH_3	3-F	2.3 ± 0.2	4
100	5-OCH_3	4-F	2.6 ± 0.2	32

[a]Selectivity relative to HEK293 cells.

demonstrated earlier (Table 2) that favorable R^1 substituents comprised 4-methyl (**25**), 4-chloro (**26**), 4-fluoro (**28**), or 5-methoxy (**32**). When R^2 was kept constant as 2-methyl, 3-fluoro and combined with these R^1 substituents, compounds **93**, **95**, **97**, and **99** resulted (Table 4). Here, it can be seen that for **95** this combination was beneficial with an IC_{50} of 0.47 μM and even more so for **97** with an IC_{50} of 100 nM and an improved selectivity profile as compared to **8**, while a neutral effect was observed for **93**. Although both **93** and **95** show an improved SI as compared to **8** (27.5), a 16-fold improvement in the SI was obtained when a fluorine was substituted at the 4-position (**98**), and this compound was significantly more potent than the others, with an IC_{50} of 190 nM. However, the combination involving the 5-methoxy (**99**) was detrimental to activity (IC_{50} 2.3 μM). This detrimental effect of the R^1 5-methoxy was also observed when R^2 comprised 2-methyl, 4-fluoro (**100**, IC_{50} 2.6 μM).

To investigate activity against the human pathogenic subspecies *T.b. rhodesiense*, the original hit (**8**) and a selection of analogues were tested against a panel of parasites including *T.b. rhodesiense*, *Trypanosoma cruzi*, *Leishmania donovani*, and *Plasmodium falciparum*, the causative agents of HAT, Chagas disease, leishmania, and malaria, respectively. As shown in Table 5, all of the compounds that were potent against *T.b. rhodesiense* were also potent against *T.b. brucei*. However, there was not a direct correlation, and some compounds, such as **29** and **80**, were significantly more potent against the human pathogenic species *T.b. rhodesiense* than might be expected based on their respective activities against *T.b. brucei*. Indeed, the activities of these two compounds against *T.b. rhodesiense* were very promising with respective IC_{50} values of 61 and 45 nM. In all cases, the compounds were exquisitely selective for

Table 5. Biological Activity Profile of Selected Compounds against a Parasite Panel (IC_{50}, μM)[a]

ID	*T.b. brucei*	*T.b. rhod.*[b]	*T. cruzi*[c]	*L.don.* axe[d]	*P. falc.* K1[e]	*Cytotox.* L6[f]
8	3.03	10	152	48	36	156
25	2.1	0.36	173	>133	124	146
26	2.1	0.61	168	168	88	224
29	1.7	0.061	71	>96	9.7	198
31	2.0	0.97	66	>124	91	70
70	0.89	0.61	198	>131	103	310
79	1.1	0.045	100	>103	48	193
81	0.98	0.24	187	>133	93	283
92	0.41	0.10	176	>121	17	308
94	0.90	0.64	147	>113	72	223

[a]Values are means of three experiments, ±50%. [b]*T.b. rhodesiense* strain STIB 900, bloodstream form (trypomastigotes). Melarsoprol was used as a control, IC_{50} 0.002 μg/mL. [c]*T. cruzi* Tulahaen C4 strain, amastigote stage. Benznidazole was used as a control, EC_{50} 0.38 μg/mL. [d]*L. donovani* MHOM-ET-67/L82 strain, amastigote stage. Miltefosine was used as a control, EC_{50} 0.20 μg/mL. [e]*P. falciparum* 3D7 strain, erythrocytic stage. Chloroquine was used as a control, EC_{50} 0.11 μg/mL. [f]Rat skeletal myoblast cell L-6 strain. Podophylotoxin was used as a control, EC_{50} 0.007 μg/mL.

T. brucei over the other parasites, and they were largely noncytotoxic with respect to the L6 mammalian cell line.

An assessment of drug-likeness was then made, and various physicochemical and metabolic parameters for selected compounds are listed in Table 6. It can be seen that all compounds are of relatively low molecular weight in the range 226−312 $gmol^{-1}$. Their polar surface areas are low and well within the range where good CNS penetration is plausible.[21] An in silico prediction model for the potential for CNS exposure was employed to further assess this possibility.[22] Of the 14 compounds screened, seven were predicted to have high CNS exposure (nominally defined as a brain to plasma ratio >0.3), and a further two (**41** and **93**) had values just below the nominal cutoff for high CNS penetration. On the basis of these predictions, this class would be expected to have reasonable CNS exposure, which could potentially lead to the treatment of the CNS stage of HAT. That said, CNS penetration is a very complex phenomenon, given that exposure depends on a number of factors including protein binding, influx and efflux, and metabolism,[23] and an in vivo assessment of these compounds is still required. Likewise, distribution coefficients were favorable in the range 2.3−4.7 at pH 7.4. Aqueous solubility for some compounds was very good; for example, both **42** and **79** had solubilities of greater than 100 μg/mL at both pH 2 and 6.5. This system was strongly influenced by the attached substituents such that **29** was very poorly soluble at 1.6−3.1 μg/mL at pH 2 and <1.6 μg/mL at pH 6.5. Plasma protein binding also varied significantly but was acceptable. Microsomal degradation was moderate to quite high across all compounds tested. Compound **29** was relatively metabolically stable with a predicted E_H value of 0.51. For this compound, the pyridine ring is substituted in the 4-position, and it is possible that the effect is to hinder metabolic oxidation of the adjacent electron-rich 6-position, which is para to the amide group. This hypothesis is supported by the observation that the most metabolically stable compound is **32** with a predicted E_H of 0.47, where the 5-position is blocked by a methoxy group.

The metabolism of compounds **34** and **95** was examined in greater detail in an effort to determine the key sites of

dx.doi.org/10.1021/jm500191u | J. Med. Chem. XXXX, XXX, XXX−XXX

Table 6. Key Physicochemical Parameters and in Vitro Metabolic Stability of Selected Compounds

ID	MW	PSA (Å^2)[a]	log D[b] pH 7.4	solubility (μg/mL)[c] pH 2	solubility (μg/mL)[c] pH 6.5	cPPB[d] (%)	in vitro CLint (μL/min/mg protein)[e]	microsome-predicted E_H	predicted CNS exposure
22	237	65.8	3.9	6.3−12.5	6.3−12.5	97.6	rapid non-NADPH mediated metabolism		high
23	237	65.8	2.8	50−100	25−50	64.1	82	0.76	high
25	226	42.0	2.8	>100	25−50	70.1	129	0.83	high
26	247	42.0	3.4	25−50	12.5−50	86.6	128	0.84	high
29	312	42.0	4.7	1.6−3.1	<1.6	98.3	27	0.51	high
32	242	51.2	2.5	>100	12.5−25	60.1	23	0.47	low
34	230	42.0	2.7	25−50	25−50	56.0	43	0.63	low
36	237	65.8	3.9	6.3−12.5	6.3−12.5	97.5	rapid non-NADPH mediated metabolism		high
41	230	42.0	3.0	>100	>100	67.0	191	0.88	low[f]
70	230	42.0	2.6	50−100	25−50	67.9	58	0.69	low
79	291	42.0	3.2	>100	>100	88.1	97	0.79	low
92	248	42.0	2.8	50−100	25−50	63.9	154	0.86	low
93	244	42.0	3.5	>100	25−50	72.4	237	0.90	low[f]
95	265	42.0	2.3	12.5−25	12.5−25	71.7	254	0.91	high

[a]Calculated using ACD/Laboratories software, version 9. [b]Measured chromatographically. [c]Kinetic solubility determined by nephelometry. [d]Human plasma protein binding estimated using a chromatographic method. [e]In vitro intrinsic clearance determined in human liver microsomes and predicted hepatic extraction ratio calculated from in vitro data. [f]Predicted B:P values of 0.28, that is, just beneath the nominal cutoff value for high CNS exposure.

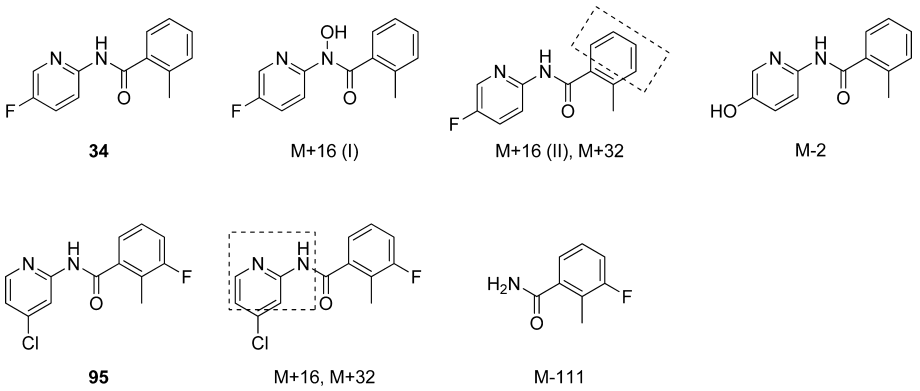

Figure 5. Structures of putative metabolites of **34** and **95**. The dotted lines indicate proposed sites of hydroxylation.

metabolism. Metabolism of **34** (Figure 5) in NADPH-supplemented human microsomal incubations revealed two mono-oxygenated metabolites (M+16 (I), *N*-hydroxylation of the amide bond; and M+16 (II), aromatic hydroxylation of the tolyl ring) and one bis-oxygenation metabolite (M+32, dihydroxylation of the tolyl moiety). A putative metabolite with a molecular ion consistent with oxidative defluorination (M−2) was also detected; however, the MS/MS signal was too weak to confirm the structure. In the presence of the dual cofactors, NADPH and UDPGA, limited glucuronidation of M +16 (II) and M+32 was observed, while in an incubation devoid of cofactors, no metabolites were detected, suggesting that NADPH-mediated hydroxylation to M+16 (I) and (II) represents the primary metabolic pathways.

Compound **95** was shown to exhibit a high rate of degradation in NADPH-supplemented human liver microsomes (Table 6), and mono-oxygenated (M+16, oxygenation of the aminopyridine moiety) and bis-oxygenated (M+32, bis-oxygenation of the aminopyridine moiety) species were identified (Figure 5). In addition, a putative metabolite with a molecular ion consistent with *N*-dearylation (M−111) was detected; however, the MS/MS signal was too weak to confirm the structure (Figure 5). In the presence of NADPH and UDPGA, extensive glucuronidation of the M+16 and M+32 metabolites was observed (i.e., there was a significant decrease in the detection of M+16 and M+32 species in conjunction with the appearance of their respective glucuronide conjugates), while in microsomal samples devoid of cofactors only a very small peak (in terms of peak area response) for the M+16 metabolite was seen, suggesting that this metabolite is likely to be formed via NADPH and, to a lesser extent, non-NADPH-dependent mechanisms. Overall, oxygenation of the amino-pyridine region appears to be the major metabolic pathway of **95**.

Comparing the metabolite profiles of **34** and **95**, the introduction of an aromatic fluorine (as in **95**) appeared to reduce the susceptibility of that region to metabolism. However, both compounds were still highly metabolized in the regions without fluorine substitution.

Another important parameter in assessing the therapeutic potential of compounds that inhibit growth of trypanosomes, or indeed any pathogenic parasite, is whether the compounds actually kill the organism or temporarily inhibit their growth. Those that are not cidal are generally viewed with less interest as potential therapeutics. It was therefore determined whether

dx.doi.org/10.1021/jm500191u | J. Med. Chem. XXXX, XXX, XXX−XXX

these compounds were trypanocidal or trypanostatic using cidal assays, and the results are shown in Table 7.

Table 7. Percentage of *T.b. brucei* Trypanosomes Killed Following Exposure to Compounds over a 72 h Period

	percentage of cells killed					
ID	24 h	STDEV	48 h	STDEV	72 h	STDEV
92	92	6.08	99.95	0.07	99.9	0
95	64.23	8.73	83.7	2.40	98.8	0.85
pentamidine	58.1		100		100	
puromycin	100		100		100	
DMSO	0		0		0	

The percentage of *T.b. brucei* trypanosomes killed following 24, 48, and 72 h exposure to the MIC of **92** and **95** as compared to the untreated DMSO control is shown in Table 7. After 24 h incubation with compounds **92** and **95**, the number of viable trypanosomes was reduced by >90 and 60%, respectively. Following further 24 h incubation, only a small population of viable trypanosomes remained (<20%), and by 72 h, >98.5% of the trypanosomes had been killed. The continual decrease and almost complete elimination of viable trypanosomes following 72 h exposure to the MIC of **92** and **95** indicates that the compounds are trypanocidal. No viable trypanosomes were detected following 24 and 48 h incubation with puromycin and pentamidine, respectively.

CONCLUSIONS

We have described the discovery of a class of pyridyl benzamides that are novel inhibitors of *T.b. brucei* and *T.b. rhodesiense*. For compound **79**, the IC_{50} value against the human pathogenic subspecies, *T.b. rhodesiense*, was 45 nM. Assessment of predictive ADMET parameters revealed that these very low molecular weight compounds have very favorable properties for further optimization. In particular, they have relatively low log *D* values, good aqueous solubility, and low plasma protein binding. Most of the analogues were predicted to have good CNS penetration, a key feature for the treatment of second stage HAT. These compounds were determined to be cidal and not static in their biological action. Ten compounds have been tested against a panel of parasites, including *T.b. rhodesiense*, alongside *T. cruzi*, *P. falciparum*, and *L. donovani*, and were shown to demonstrate selectivity toward *T. brucei* in comparison to the other trypanosome species. These compounds did not display significant activity against L6 cells. Improvement of the metabolic stability of these compounds will be a key parameter to optimize during the next phase of development.

While an efficacy study for these compounds has not yet been undertaken, it is an important proof of principle experiment. Given the expense associated with using an animal model for HAT and the time required to perform the experiment, further improvement in metabolism is required before these experiments are performed.

The specific biological target or targets of this series of compounds remain unknown. However, for some of the more active compounds, with whole organism IC_{50} values of less than 100 nM, it is reasonable to assume that target affinity may be in the low nanomolar range. Target identification is warranted to enable the facilitation of the next stage of rational optimization.

EXPERIMENTAL SECTION

General Chemistry Experimental. See the Supporting Information.

Determination of Purity. Purity was determined using high performance liquid chromatography (HPLC) carried out either on a Waters Auto Purification System 3100 with a Waters column (XBridgePrep C18, 5 μm, OBD, 19 × 100 mm) or on a Waters Alliance HT 2795 with a Phenomenex column (Luna, 5 μm, C18, 100 Å, 150 × 10 mm). The purity of all compounds for biological testing was >95% in all cases, except where specified otherwise.

PHYSICOCHEMICAL STUDIES

Solubility Estimates Using Nephelometry. This was obtained as described previously.[1,24] See the Supporting Information for more information.

Chromatographic Log *D* Measurement. Partition coefficients (log *D*) were estimated as described previously.[1,25] See the Supporting Information for more information.

Chromatographic Protein Binding Estimation. This was obtained as previously described.[1,26] See the Supporting Information for more information.

In Vitro Metabolism in Human Liver Microsomes. Data were obtained as described previously.[1,27,28] See the Supporting Information for more information.

Metabolite ID. Each test compound was incubated at 37 °C with human liver microsomes (XenoTech, lot no. 1210057), and the reaction was initiated by the addition of an NADPH-regenerating system as described above. To maximize the metabolite yield, a high substrate concentration (10 μM) and high microsomal protein concentration (1 mg/mL) were used, and incubations were conducted for up to 60 min. Samples without test compound and without NADPH were included as controls. In addition, a single sample initiated by the addition of the dual cofactor system (containing the NADPH regeneration buffer described and UDPGA (mixture A, BD Gentest) in the presence of 0.025 mg/mL alamethacin) was included (at the 60 min time point) for the qualitative assessment of the potential for glucuronide formation. Reactions were quenched by protein precipitation with an equal volume of ice-cold acetonitrile (containing 0.15 μg/mL diazepam as internal standard), and then centrifuged for 3 min at 10000 rpm. The supernatant was removed and analyzed for parent degradation and metabolite formation by LC/MS (Waters Micromass Xevo G2 QTOF coupled to a Waters Acquity UPLC). The mobile phase consisted of an acetonitrile−water gradient (containing 0.05% formic acid). A Supelco Ascentis Express RP-Amide (50 × 2.1 mm) column was used. MS analyses were conducted in positive mode electrospray ionization under MSE acquisition mode, which allows simultaneous acquisition of MS spectra at low and high collision energies. The identity of putative metabolites was confirmed by accurate mass and MS/MS fragmentation where possible.

In Silico Prediction of CNS Exposure. The partial least-squares projection to latent structures (PLS) model developed for CNS exposure in 2012[22] was applied to 14 representative compounds. SMILES strings were submitted to the software Corina 3.0 (Molecular Networks, Erlangen, Germany) to produce the three-dimensional structures. The resulting structures were used to calculate a large number of physicochemical properties and molecular descriptors using DragonX (Talete, Italy). These descriptors were then submitted to the PLS model, and the CNS exposure was predicted. On the basis of the predicted brain to plasma (B:P)

dx.doi.org/10.1021/jm500191u | J. Med. Chem. XXXX, XXX, XXX−XXX

value, the compounds were classified as showing high CNS exposure (B:P > 0.3) or low CNS exposure (B:P < 0.3).

BIOLOGICAL ASSAYS

All in vitro assays were carried out at least twice independently in singleton. The IC_{50} values are the means of two independent assays and vary by less than ±50%.

***P. falciparum* Assay.** This was undertaken as previously described.[1,29−32] See the Supporting Information for more information.

***L. donovani* Axenic Amastigotes Assay.** This was undertaken as previously described.[1,32−34] See the Supporting Information for more information.

***T. cruzi* Assay.** Data were obtained as previously described.[1,32,35] See the Supporting Information for more information.

***T. brucei rhodesiense* Assay.** This was undertaken as previously described.[1,32,36,37] See the Supporting Information for more information.

Rat Skeletal Myoblast Cytotoxicity Assay. This was undertaken as previously described.[1,32,38,39] See the Supporting Information for more information.

***T.b. brucei* Assay.** This was undertaken as previously described.[1,40,41] See the Supporting Information for more information.

HEK293 Cytotoxicity Assay. This was undertaken as previously described.[1] See the Supporting Information for more information.

Cidal Assay. The number of viable trypanosomes remaining following 24, 48, and 72 h exposure to the minimum inhibitory concentration (MIC) of compounds was determined by directly visualizing and counting the number of parasites present at each time point. The assay was performed as described previously in detail by Sykes et al.[13] Briefly, 55 μL of *T.b. brucei* parasites was added to a black/clear bottomed 384 well microtiter plate and incubated for 24 h at 37 °C/5% CO_2. Compounds were diluted in DMEM medium, and 5 μL of this dilution was added to assay plates to give the MIC. After 24, 48, and 72 h incubation at 37 °C/5% CO_2, wells were directly visualized under a microscope, and the number of parasites remaining was determined by counting a sample of the wells in a hemocytometer. The cell counts were compared to that of the positive control, puromycin (MIC1.15 μM), and the negative control DMSO (0.4%), and the percentage of trypanosomes killed was subsequently determined. The MIC of each compound was defined as the minimum concentration at which there was a plateau of activity in the Alamar blue assay (>95% activity). The experiment was performed in duplicate.

ASSOCIATED CONTENT

Supporting Information

Experimental procedures for compound synthesis and characterization. This material is available free of charge via the Internet at http://pubs.acs.org.

AUTHOR INFORMATION

Corresponding Author

*Tel.: +61 9903 9044. E-mail: Jonathan.Baell@monash.edu.

Author Contributions

□L.F. and M.G. contributed equally.

Notes

The authors declare no competing financial interest.

ACKNOWLEDGMENTS

This research was supported by the NHMRC (IRIISS grant number 361646; NHMRC Senior Research Fellowship 1020411 (J.B.B.), NHMRC Project Grant 1025581); Victorian Stage Government OIS grant; the Australian Government for the Australian Postgraduate Award (L.F.); Dr. Jason Dang for his assistance in obtaining some of the analytical data; and DNDi for allowing access to their parasite screening platform at STPHI.

ABBREVIATIONS USED

CNS, central nervous system; HAT, human African trypanosomiasis; T.b. brucei, *Trypanosoma brucei* brucei; T.b. gambiense, *Trypanosoma brucei* gambiense; T.b. rhodesiense, *Trypanosoma brucei* rhodesiense

REFERENCES

(1) WHO. Control and surveillance of human African trypanosomiasis. http://apps.who.int/iris/bitstream/10665/95732/1/9789241209847_eng.pdf (accessed, 10th January, 2014).

(2) Brun, R.; Blum, J.; Chappuis, F.; Burri, C. Human African trypanosomiasis. *Lancet* **2010**, *375*, 148−159.

(3) WHO. Drugs. http://www.who.int/trypanosomiasis_african/drugs/en/index.html (accessed, July 27, 2012).

(4) Voogd, T. E.; Vansterkenburg, E. L.; Wilting, J.; Janssen, L. H. Recent research on the biological activity of suramin. *Pharmacol. Rev.* **1993**, *45*, 177−203.

(5) de Koning, H. P. Transporters in African trypanosomes: role in drug action and resistance. *Int. J. Parasitol.* **2001**, *31*, 512−522.

(6) Nok, A. J. Arsenicals (melarsoprol), pentamidine and suramin in the treatment of human African trypanosomiasis. *Parasitol. Res.* **2003**, *90*, 71−79.

(7) Seebeck, T.; Maser, P. Drug resistance in African Trypanosomiasis. In *Antimicrobial Drug Resistance*; Mayers, D. L., Ed.; Humana Press: Totowa, NJ, 2009; pp 589−604.

(8) Priotto, G.; Kasparian, S.; Mutombo, W.; Ngouama, D.; Ghorashian, S.; Arnold, U.; Ghabri, S.; Baudin, E.; Buard, V.; Kazadi-Kyanza, S.; Ilunga, M.; Mutangala, W.; Pohlig, G.; Schmid, C.; Karunakara, U.; Torreele, E.; Kande, V. Nifurtimox-eflornithine combination therapy for second-stage African *Trypanosoma brucei gambiense* trypanosomiasis: a multicentre, randomised, phase III, non-inferiority trial. *Lancet* **2009**, *374*, 56−64.

(9) Barrett, M. P. Potential new drugs for human African trypanosomiasis: some progress at last. *Curr. Opin. Infect. Dis.* **2010**, *23*, 603−608.

(10) DNDi. New Oral Drug Candidate for African Sleeping Sickness. http://www.dndi.org/media-centre/press-releases/354-media-centre/press-releases/1505-new-oral-drug-candidate-hat.html (accessed, 9th July).

(11) DNDi. Oxaborole SCYX-7158 (HAT). http://www.dndi.org/portfolio/oxaborole-scyx-7158.html (accessed, July 27, 2012).

(12) Ferrins, L.; Rahmani, R.; Baell, J. B. Drug discovery and human African trypanosomiasis: a disease less neglected? *Future Med. Chem.* **2013**, *5*, 1801−1841.

(13) Sykes, M. L.; Baell, J. B.; Kaiser, M.; Chatelain, E.; Moawad, S. R.; Ganame, D.; Ioset, J.-R.; Avery, V. M. Identification of Compounds with Anti-Proliferative Activity against *Trypanosoma brucei brucei* Strain 427 by a Whole Cell Viability Based HTS Campaign. *PLoS Neglected Trop. Dis.* **2012**, *6*, e1896.

(14) Ferrins, L.; Rahmani, R.; Sykes, M. L.; Jones, A. J.; Avery, V. M.; Teston, E.; Almohaywi, B.; Yin, J.; Smith, J.; Hyland, C.; White, K. L.; Ryan, E.; Campbell, M.; Charman, S. A.; Kaiser, M.; Baell, J. B. 3-(Oxazolo[4,5-*b*]pyridin-2-yl)anilides as a novel class of potent inhibitors for the kinetoplastid *Trypanosoma brucei*, the causative agent for human African trypanosomiasis. *Eur. J. Med. Chem.* **2013**, *66*, 450−465.

(15) White, G. A. Substituted benzanilides: Structural variation and inhibition of complex II activity in mitochondria from a wild-type strain and a carboxin-selected mutant strain of Ustilago maydis. *Pestic. Biochem. Physiol.* **1987**, *27*, 249−260.
(16) Turrens, J. F. The role of succinate in the respiratory chain of Trypanosoma brucei procyclic trypomastigotes. *Biochem. J.* **1989**, *259*, 363−368.
(17) Zeiman, E.; Greenblatt, C. L.; Elgavish, S.; Khozin-Goldberg, I.; Golenser, J. Mode of action of fenarimol against Leishmania spp. *J. Parasitol.* **2008**, *94*, 280−286.
(18) Urbina, J. A.; Payares, G.; Molina, J.; Sanoja, C.; et al. Cure of short- and long-term experimental Chagas' disease using D0870. *Science* **1996**, *273*, 969−971.
(19) Gamo, F.-J.; Sanz, L. M.; Vidal, J.; de Cozar, C.; Alvarez, E.; Lavandera, J.-L.; Vanderwall, D. E.; Green, D. V. S.; Kumar, V.; Hasan, S.; Brown, J. R.; Peishoff, C. E.; Cardon, L. R.; Garcia-Bustos, J. F. Thousands of chemical starting points for antimalarial lead identification. *Nature* **2010**, *465*, 305−310.
(20) Meanwell, N. A. Synopsis of some recent tactical application of bioisosteres in drug design. *J. Med. Chem.* **2011**, *54*, 2529−2591.
(21) Pajouhesh, H.; Lenz, G. R. Medicinal chemical properties of successful central nervous system drugs. *NeuroRx* **2005**, *2*, 541−53.
(22) Bergström, C. S.; Charman, S.; Nicolazzo, J. Computational prediction of CNS drug exposure based on a novel in vivo dataset. *Pharm. Res.* **2012**, *29*, 3131−3142.
(23) Di, L.; Rong, H.; Feng, B. Demystifying brain penetration in central nervous system drug discovery. *J. Med. Chem.* **2012**, *56*, 2−12.
(24) Bevan, C. D.; Lloyd, R. S. A high-throughput screening method for the determination of aqueous drug solubility using laser nephelometry in microtiter plates. *Anal. Chem.* **2000**, *72*, 1781−1787.
(25) Lombardo, F.; Shalaeva, M. Y.; Tupper, K. A.; Gao, F. ElogDoct: A tool for lipophilicity determination in drug discovery. 2. Basic and neutral compounds. *J. Med. Chem.* **2001**, *44*, 2490−2497.
(26) Valko, K.; Nunhuck, S.; Bevan, C.; Abraham, M. H.; Reynolds, D. P. Fast gradient HPLC method to determine compounds binding to human serum albumin. Relationships with octanol/water and immobilized artificial membrane lipophilicity. *J. Pharm. Sci.* **2003**, *92*, 2236−2248.
(27) Obach, R. S. Prediction of human clearance of twenty-nine drugs from hepatic microsomal intrinsic clearance data: An examination of *in vitro* half-life approach and nonspecific binding to microsomes. *Drug Metab. Dispos.* **1999**, *27*, 1350−1359.
(28) Davies, B.; Morris, T. Physiological parameters in laboratory animals and humans. *Pharm. Res.* **1993**, *10*, 1093−1095.
(29) Desjardins, R. E.; Canfield, C. J.; Haynes, J. D.; Chulay, J. D. Quantitative assessment of antimalarial activity *in vitro* by a semiautomated microdilution technique. *Antimicrob. Agents Chemother.* **1979**, *16*, 710−718.
(30) Matile, H.; Pink, J. R. L. *Plasmodium falciparum* malaria parasite cultures and their use in immunology. In *Immunological Methods*; Lefkovits, I., Pernis, B., Eds.; Academic Press: San Diego, CA, 1990.
(31) Ponnudurai, T.; Leeuwenberg, A. D.; Meuwissen, J. H. Chloroquine sensitivity of isolates of *Plasmodium falciparum* adapted to *in vitro* culture. *Trop. Geogr. Med.* **1981**, *33*, 50−54.
(32) Huber, W.; Koella, J. C. A comparison of three methods of estimating EC_{50} in studies of drug resistance of malaria parasites. *Acta Trop.* **1993**, *55*, 257−261.
(33) Cunningham, M. L.; Fairlamb, A. H. Trypanothione reductase from *Leishmania donovani*. Purification, characterisation and inhibition by trivalent antimonials. *Eur. J. Biochem.* **1995**, *230*, 460−468.
(34) Mikus, J.; Steverding, D. A simple colorimetric method to screen drug cytotoxicity against Leishmania using the dye Alamar Blue. *Parasitol. Int.* **2000**, *48*, 265−269.
(35) Buckner, F. S.; Verlinde, C. L.; La Famme, A. C.; CVan Voorhis, W. C. Efficient technique for screening drugs for activity against *Trypanosoma cruzi* using parasites expressing beta-galactosidase. *Antimicrob. Agents Chemother.* **1996**, *40*, 2592−2597.
(36) Baltz, T.; Baltz, D.; Giroud, C.; Crockett, J. Cultivation in a semi-defined medium of animal infective forms of *Trypanosoma brucei*, *T. equiperdum*, *T. evansi*, *T. rhodesiense* and *T. gambiense*. *EMBO J.* **1985**, *4*, 1273−1277.
(37) Räz, B.; Iten, M.; Grether-Bühler, Y.; Kaminsky, R.; Brun, R. The Alamar Blue assay to determine drug sensitivity of African trypanosomes (*T.b. rhodesiense* and *T.b. gambiense*) *in vitro*. *Acta Trop.* **1997**, *68*, 139−147.
(38) Page, B.; Page, M.; Noel, C. A new fluorometric assay for cytotoxicity measurements *in vitro*. *Int. J. Oncol.* **1993**, *3*, 473−476.
(39) Ahmed, S. A.; Gogal, R. M.; Walsh, J. E. A new rapid and simple non-radioactive assay to monitor and determine the proliferation of lymphocytes: an alternative to [3*H*]thymidine incorporation assay. *J. Immunol. Methods* **1994**, *170*, 211−224.
(40) Sykes, M. L.; Avery, V. M. Development of an Alamar blue viability assay in 384-well format for high throughput whole cell screening of *Trypanosoma brucei brucei* bloodstream form strain 427. *Am. J. Trop. Med. Hyg.* **2009**, *81*, 665−674.
(41) Hirumi, H.; Hirumi, K. Continuous cultivation of *Trypanosoma brucei* blood stream forms in a medium containing a low concentration of serum protein without feeder cell layers. *J. Parasitol.* **1989**, *75*, 985−989.